coatings

MDPI

Article

Impact of Water-Repellent Products on the Moisture Transport Properties and Mould Susceptibility of External Thermal Insulation Composite Systems

Renata Roncon [1], Giovanni Borsoi [1,*], João L. Parracha [1,2], Inês Flores-Colen [1], Rosário Veiga [2] and Lina Nunes [3,4]

1 CERIS, Civil Engineering Research and Innovation for Sustainability, Instituto Superior Técnico, University of Lisbon, 1049-001 Lisbon, Portugal; renata.roncon@tecnico.ulisboa.pt (R.R.); jparracha@lnec.pt (J.L.P.); ines.flores.colen@tecnico.ulisboa.pt (I.F.-C.)
2 Buildings Department, LNEC, National Laboratory for Civil Engineering, 1700-066 Lisbon, Portugal; rveiga@lnec.pt
3 Structures Department, LNEC, National Laboratory for Civil Engineering, 1700-066 Lisbon, Portugal; linanunes@lnec.pt
4 cE3c, Centre for Ecology, Evolution and Environmental Changes, Azorean Biodiversity Group, University of Azores, 9700-042 Azores, Portugal
* Correspondence: giovanni.borsoi@tecnico.ulisboa.pt; Tel.: +351-218443975

Abstract: External Thermal Insulation Composite Systems (ETICS) are constructive solutions widely used to increase the thermal insulation in new and retrofitted buildings. However, these systems can present several anomalies due to their constant exposure to weathering agents and anthropic factors. Water is generally the major cause of degradation. Thus, the application of water-repellent products can minimize the appearance of anomalies and increase the durability of the systems. In this paper, acrylic-based and siloxane-based hydrophobic products were applied to ETICS, with the aim of assessing the compatibility, effectiveness, and durability of these products. The moisture transport properties and mould susceptibility were assessed through laboratory tests on untreated and treated specimens. The durability of the hydrophobic treatments was also evaluated through artificial aging tests (heat-cold and freeze-thaw cycles). Results show that the protection products generally decreased water absorption, slightly decreased the drying rate, and presented adequate water vapor permeability. After aging, the products still had reasonable effectiveness and, with one exception, improved the water vapor diffusion of the systems. Additionally, ETICS underwent an alteration in the finishing coat (possible modification of the porosity) due to the aging cycles. No clear linear correlation was found between the contact angle values and water absorption results, evidencing the influence of other factors related to the composition of the water-repellent products.

Keywords: ETICS; hydrophobic protection; water-repellency; moisture transport properties; mould susceptibility; durability

Citation: Roncon, R.; Borsoi, G.; Parracha, J.L.; Flores-Colen, I.; Veiga, R.; Nunes, L. Impact of Water-Repellent Products on the Moisture Transport Properties and Mould Susceptibility of External Thermal Insulation Composite Systems. *Coatings* **2021**, *11*, 554. https://doi.org/10.3390/coatings11050554

Academic Editor: Fabio Palumbo

Received: 6 April 2021
Accepted: 5 May 2021
Published: 8 May 2021

1. Introduction

The optimization of energy efficiency associated with the building environment has been gaining a growing interest in the construction industry also due to new regulations of the European Union [1]. In this context, External Thermal Insulation Composite Systems (ETICS), which significantly improve the thermal performance of building walls both in new construction and retrofitting interventions [2], have been extensively applied.

However, the ETICS can present several anomalies (e.g., stains, cracks, biological colonization) due to their constant exposure to weathering agents and anthropic factors, which can compromise their thermal performance and long-term durability. Water is generally among the main decay agents, often triggering physical-mechanical-chemical degradation and favoring biological growth [2,3]. For this reason, the application of multifunctional

protective coatings with hydrophobic properties can minimize the appearance of anomalies and, at the same time, increase the long-term durability of the ETICS by reducing the wettability and water absorption of the treated substrate.

Water repellent products can be classified as film-formers or penetrants. Film formers can either act as a coating, developing a continuous film on the surface (i.e., paints and varnishes), or as a pore blocker, penetrating into the substrate and filling the superficial pores [4,5]. On the other hand, penetrants enter in-depth in the pores of the material and create a hydrophobic film within the porous network [4]. The main difference between film formers and penetrants is related to the alteration of the water vapor permeability of the substrate. In fact, the application of penetrants generally does not alter the porous network; thus, the water vapor diffusion is almost unaffected. In the case of film formers and pore blocker products, water vapor permeability is significantly affected by pore-filling [5].

The change in water vapor permeability and drying kinetics can contribute to speeding up the degradation of the material; thus, the comprehension of the effect of water-repellent products on the moisture transport properties of the ETICS is a critical task [6]. Furthermore, the effectiveness of these products depends not only on their chemical properties but also on the physical features of the substrate [7,8]. Previous studies reported an aesthetical alteration and reduction in water vapor permeability as a consequence of the application of the hydrophobic products; thus, a deeper comprehension of the action of these products when applied to the ETICS is needed. Additionally, the selected water-repellent products need suitable durability in order to provide long-lasting protection against degradation agents (e.g., water, ultraviolet (UV) radiation, pollutants) [3,8].

Previous studies analyzed the influence of different water-repellent products on the performance of several building materials, such as stone [6], concrete [5,9], mortars [10], and renders [3,4]. However, only few researches evaluated the performance and durability of film former hydrophobic products on the ETICS [4,7].

Esteves et al. [7] evaluated the influence of three silicon-based hydrophobic products on the moisture transport properties and mould susceptibility of the ETICS. The results showed a decrease between 95% and 98% in the capillary water absorption after the application of the products. The results of the water vapor permeability suggested that the permeability of the ETICS can be reduced in the range of 4–21% with the application of hydrophobic products. Although the biological susceptibility of the systems was not significantly affected after the application of the products, the durability of the hydrophobic protection products was not evaluated in the study.

The present study aims to evaluate the compatibility, effectiveness, and durability of three different commercial film-former hydrophobic products (two acrylic-based and one siloxane-based) when applied on ETICS. The moisture transport properties (capillary water absorption, water absorption under low pressure, drying kinetics, water vapor permeability, and contact angle) and the susceptibility to mould development were assessed through laboratory tests on treated and untreated specimens. The durability of the treatments was also assessed through artificial aging tests (heat-cold and freeze-thaw cycles). The moisture transport properties and the mould susceptibility of the specimens were assessed before and after the selected aging cycles.

2. Materials and Methods

2.1. Materials

2.1.1. ETICS Specimens

The ETICS specimens consist of an expanded polystyrene (EPS) thermal insulation board (with a thickness of ~40 mm), a cement base coat (2.22 $\pm$ 0.03 mm), which incorporates a glass fiber mesh, and an acrylic-based finishing coat (0.57 $\pm$ 0.06 mm), with some hydrophobic and biocide properties. The selected ETICS has a European Technical Assessment (ETA) and, thus, fulfills the performance requirements of EAD 040083-00-0404 [11].

2.1.2. Hydrophobic Protection Products

Three different commercially available waterborne protection products (H1, H2, and H3) were selected based on market research. These products were selected considering different chemical compositions, thus possibly affecting their compatibility, effectiveness, and durability when applied to ETICS.

Products H1 and H3 are acrylic-based and present TiO_2 and ZnO (which can be used as white pigments or photocatalytic additives), calcium carbonate (white pigment and filler), and biocide additives in their compositions (mix of 2/3 biocide e.g., isothiazolinone, terbutryn). H3 also consists of low percentages of further acrylates (i.e., diisobutyrate, butyl acrylate, methyl methacrylate), whereas H1 also has zinc pyrithione (further biocide additive). H2 is a siloxane-based product, which contains TiO_2 and ZnO (pigments or photocatalytic additives), magnesium and calcium carbonate (white pigment and filler), and biocide additives in its composition (mix of 3 biocides e.g., isothiazolinone, terbutryn).

Table 1 presents the identification and some features of the three commercially available waterborne protection products considered in this study (Figure 1a).

Table 1. Physical features and application protocol of the hydrophobic protection products.

Product Identification	Color	pH	Density (g/cm^3) at T = 20 °C and RH = 60%	Dry Residue (g/L)	Amount of Product per Application (L/m^2)
H1	Whitish	8.5	1.34 ± 0.05	737	2 applications: 1st coat: 0.13; 2nd coat: 0.12
H2	Whitish	9.25	1.58 ± 0.05	1051	
H3	Whitish	8.5	1.30 ± 0.03	729	

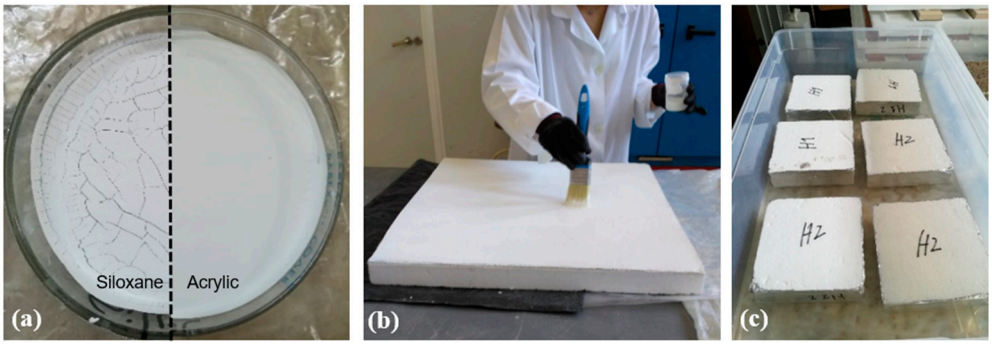

Figure 1. (**a**) Dry residue of H2 (siloxane) and H3 (acrylic-based paint); (**b**) application of product on ETICS board; (**c**) capillary water absorption test on ETICS specimens.

2.2. Methods

2.2.1. Application Protocol

The application of the three products (H1, H2, and H3) was carried out by brush on the ETICS boards, following the recommendations of the manufacturers (Figure 1b, Table 1). Two coats of the product were applied per board (Table 1) in orthogonal directions. The first coat was diluted in 10% distilled water. A drying time of 24 h between coat application was considered in order to guarantee the complete evaporation of the aqueous solvent. The treated ETICS boards were then kept in controlled environmental conditions (T = 20 ± 2 °C and 50% ± 5% RH) for 7 days.

2.2.2. Specimens

According to the tests performed, specimens with different dimensions were cut from the treated ETICS boards. Prismatic specimens, with dimension 150 mm × 150 mm (42.5–43 mm thickness), were used for water absorption tests (by capillarity and under low pressure) and drying tests. Cylindrical specimens with a diameter of ~7.2 cm (42.5–43 mm thickness) were used for water vapor permeability and contact angle measurement. Fur-

thermore, smaller prismatic specimens (40 mm × 40 mm × (42.5–43) mm thickness) were used to assess biological susceptibility to moulds. Untreated specimens (H0) were also considered as a reference. A metallic scotch tape was used to seal the lateral side of the thermal insulation of the systems to avoid water penetration within the insulation during both capillary water absorption and artificial aging tests, and also to facilitate the handling of the specimens during the experimental campaign.

2.2.3. Moisture Transport Properties

Tests were carried out threefold in treated (with water-repellent products) and untreated specimens.

The capillarity water absorption test was carried out under controlled conditions (65% RH, T = 20 °C, airspeed < 0.1 m/s), according to EAD 040083-00-0404 [11] (Figure 1c). Specimens were laterally sealed using waterproof scotch tape to avoid water penetration within the thermal insulation. The capillary water absorption coefficient (*Cc*) was determined by the initial slope of the capillary absorption curve and was calculated according to Equation (1).

$$Cc = \frac{M_2 - M_1}{A \times \left(\sqrt{0.05}\right)} \quad (1)$$

where *Cc* is the capillary water absorption coefficient (kg/(m^2·h$^{0.5}$)); M_1 is the mass of the specimen at the beginning of the test (kg); M_2 is the mass of the specimen after 3 min (kg); A is the immersed base area (m^2).

The drying test was performed according to EN 1 6322 [12] and started immediately after the end of the capillarity water absorption test, using the same test specimens and controlled conditions. The drying kinetics were evaluated through the results obtained for the first drying rate (DR_1 in kg/(m^2·h)), the second drying rate (DR_2 in (kg/(m^2·h$^{0.5}$)), and the drying index (*DI*). The first drying rate corresponds to the transport of liquid water, whereas the second drying rate mainly represents vapor transport. The drying index (*DI*) is obtained according to Equation (2) [7] and reflects the global drying kinetics.

$$DI = \frac{\int_{t_0}^{t_f} f\left(\frac{M_x - M_1}{M_1}\right) \mathrm{d}t}{\left(\frac{M_3 - M_1}{M_1}\right) \times t_f} \quad (2)$$

being M_x the specimen mass registered during the drying process (g); M_1 the specimen mass in the dry state (g); M_3 the specimen mass at the beginning of the test (g); t_f the ending time of the drying process (h).

Water absorption under low pressure using Karsten tubes was performed according to test No. II.4 of RILEM [13]. Two Karsten tubes for horizontal surfaces were applied to each specimen. Water absorption was monitored for 24 h, in order to have results comparable with those of the capillarity water absorption test. The water absorption coefficient at 60 min was determined following Equation (3).

$$C_{abs}^{60min} = \frac{A_{bp} \times 10^{-3}}{A_{contact} \times 10^{-4} \times \sqrt{60}} \quad (3)$$

where, C_{abs}^{60min} is the coefficient of water absorption at 60 min (kg/(m^2·h$^{0.5}$)); A_{bp} is the water mass absorbed after 60 min (g); $A_{contact}$ is the contact area of the tube with the surface (≈ 5.7 cm^2).

The contact angle was measured by the sessile drop technique, i.e., Axisymmetric Drop Shape Analysis. This test is based on the variation of the interface free energy (area/water drop) and was carried out by dropping 4 ± 0.4 µL of water with a micropipette on each specimen. The images of the water drop were registered using a video camera (jAi CV-A50, Copenhagen, Denmark), mounted on a microscope Wild M3Z (Leica Microsystems,

Wetzlar, Germany), and analyzed using MATLAB (version 9.0). The contact angle was measured according to Equation (4) (using MATLAB).

$$\theta = 2 \arctan\left(\frac{2 \times hm}{am}\right) \quad (4)$$

where, θ is the static contact angle (degree); *hm* is the drop heigh (mm); *am* is the contact diameter of the microdrop (mm). Three contact angle measurements were performed per specimen, and the final result is obtained by calculating the average value of those measurements.

The water vapor permeability (WVP) test was carried out following the recommendations of EAD 040083-00-0404 [11] and EN 1015-19 [14] and using the dry cup method. The water vapor diffusion resistance coefficient (μ) was obtained using Equations (5) and (6). The equivalent air thickness (S_d) was calculated using Equation (7).

$$\Lambda = \frac{m}{A \times \Delta_p} \quad (5)$$

$$\mu = \frac{1.94 \times 10^{-10}}{\times e} \quad (6)$$

$$S_d = \mu \times e \quad (7)$$

In the above Equations, Λ is water permeance (kg/(m^2·s·Pa)); *m* is the slope of the linear relationship between mass variation and time (kg/s); *A* is the specimen area (m^2); Δ_p is the difference between the exterior and interior vapor pressure (Pa); *e* is the thickness of the specimen (m).

2.2.4. Optical Microscopy

Optical microscopy was used to observe the surface of the ETICS specimens before and after the accelerated aging test, to detect possible anomalies (e.g., microcracks, loss of surface material, chromatic changes) caused by aging, as well as evaluate surface morphology. The surfaces of the specimens were observed using a stereo microscope Olympus SZH-10 (Olympus, Tokyo, Japan) equipped with an image acquisition system Olympus SC-30 and with the software Olympus LabSens.

2.2.5. Susceptibility to Mould Growth

The susceptibility to mould growth was carried out following a method adapted from ASTM D 5590-17 (2017) [15] and ASTM C 1338-19 (2019) [16] and validated elsewhere [17]. A mixed spore suspension of *Aspergillus niger* and *Penicillium funiculosum* was prepared and uniformly applied (2 mL) to the surface of the previously steam-sterilized specimens, controls, and surrounding culture media (4% malt, 2% agar). The test flasks were then incubated for four weeks in a culture chamber (T = 22 ± 1 °C and 70% ± 5% RH).

Three replicates of Whatman n° 1 filter paper (45 mm diameter) and three wood samples (*Pinus pinaster*) with dimensions of 40 mm × 40 mm × 10 mm were used as controls, thus allowing the validation of the test [16]. The specimens and controls were visually rated for mould growth each week using the scale defined in ASTM D5590-17 [15]. At the end of the 4-week testing, specimens and controls were carefully removed from the test flasks, and the final percentage of contaminated surface was evaluated using a stereo microscope Olympus B061 (Olympus, Tokyo, Japan).

2.2.6. Accelerated Aging Test

The durability of the hydrophobic treatments was assessed through artificial aging tests with hygrothermal cycles (heat-cold and freeze-thaw). These cycles were adapted from EN 1015-21 [18], validated in previous studies [3,19], and designed to represent extreme climate conditions. Eight cycles of each type were performed. At the end of the hygrothermal cycles, specimens were stabilized for 48 h (T = 20 ± 2 °C and 50% ± 5%

RH), and the moisture transport properties and mould susceptibility of the artificially aged untreated and treated specimens were evaluated. Table 2 presents the accelerated aging test conditions.

Table 2. Accelerated aging test conditions.

Heat-Cold Cycles	Freeze-Thaw Cycles	Exposure Time
Heating-Infrared lamps (T = 60 ± 2 °C)	Sprinkler system (water at T = 20 ± 1 °C)	8 h ± 15 min
Stabilization (T = 20 ± 2 °C, RH = 65% ± 5%)	Stabilization (T = 20 ± 2 °C, RH = 65% ± 5%)	30 ± 2 min
Deep freeze cabinet (T = −15 ± 1 °C)	Deep freeze cabinet (T = −15 ± 1 °C)	15 h ± 15 min
Stabilization (T = 20 ± 2 °C, RH = 65% ± 5%)	Stabilization (T = 20 ± 2 °C, RH = 65% ± 5%)	30 ± 2 min

3. Results

3.1. Capillary Water Absorption and Water Absorption under Low Pressure

The values obtained for capillary water absorption and absorption under low pressure with Karsten tubes are presented in Figure 2 and Table 3. The results showed that with the application of the hydrophobic protection products, a decrease in the capillary water absorption coefficient (*Cc*) between 25% and 35% was obtained (Table 3), H3 being (acrylic-based) the less water absorbent treatment (Figure 2). Nevertheless, all specimens (treated and untreated) presented values of absorbed water lower than 1 kg/m^2 at 1 h of testing, as required by EAD 040083-00-0404 [11] (Figure 2).

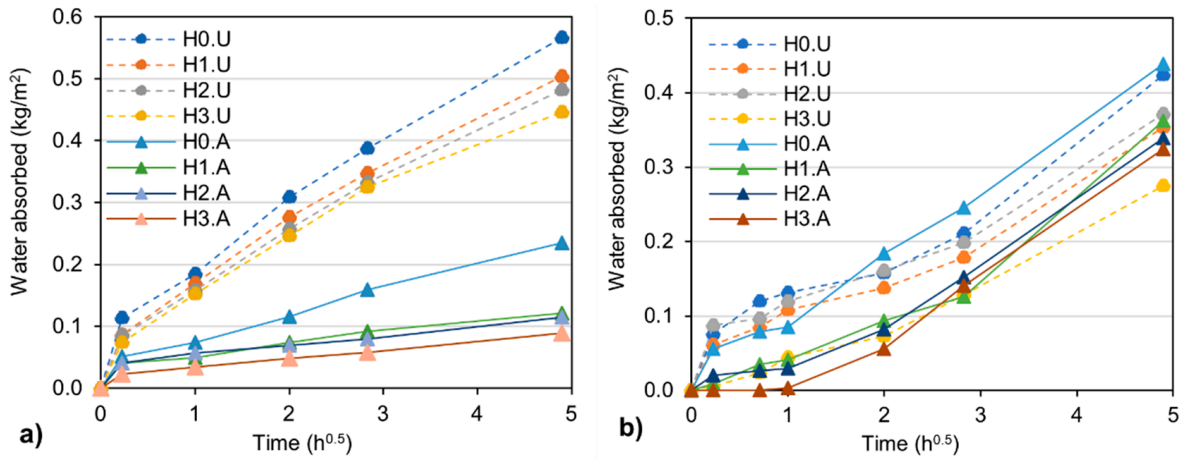

Figure 2. (**a**) Capillary water absorption curves; (**b**) water absorption curves (Karsten tube test). Notation: (U)—unaged; (A) aged specimens.

Table 3. Average results and relative standard deviation of the capillarity water absorption coefficient (*Cc*) and water absorption coefficient under low pressure (C^{60}) for protected and unprotected specimens prior to and after artificial aging test.

System	Unaged Specimens		Aged Specimens	
	Cc (kg/m^2·h$^{0.5}$)	C^{60} (kg/m^2·h$^{0.5}$)	*Cc* (kg/m^2·h$^{0.5}$)	C^{60} (kg/ m^2·h$^{0.5}$)
H0 (reference)	0.51 ± 0.04	0.13 ± 0.04	0.23 ± 0.05	0.09 ± 0.03
H1	0.38 ± 0.04	0.11 ± 0.05	0.18 ± 0.05	0.04 ± 0.04
H2	0.38 ± 0.03	0.12 ± 0.02	0.18 ± 0.02	0.03 ± 0.03
H3	0.33 ± 0.03	0.04 ± 0.03	0.10 ± 0.01	0.01 ± 0.01

The results obtained after the accelerated aging test showed that capillary water absorption decreased in all systems, including the untreated ETICS (~55% *Cc* reduction, compared to unaged specimens) (Table 3). However, the results indicated that specimens

protected with hydrophobic products continue to have enhanced water-repellent properties compared to unprotected aged specimens, showing lower *Cc* values. The highest reduction (~70%) in capillary water absorption after aging was obtained for H3.

The Karsten tube test results showed a reduction in the water absorption coefficient (C^{60}) for all systems with the applied hydrophobic products. The highest decrease (~69%) was obtained for H3, whereas a lower variation of ~15% was obtained for H1 and H2 (Table 3). These results are, therefore, in agreement with the capillary water absorption results.

As in the capillary water absorption test, the results obtained after aging showed significantly lower C^{60} values when compared to the results obtained for the treated and untreated ETICS. The highest reduction (~75%) was registered for both H2 and H3 and the lowest for H0 (~31%). Contrary to what was expected considering the capillary absorption test, Karsten tube results showed inverted trends throughout the test, with H1 and H3 (both acrylic-based) and H0 (reference) sometimes obtaining higher water absorption values after aging (Figure 2b). These results can indicate some loss of the effectiveness of the product caused by aging. Conversely, the absorption values for the aged specimens of H2 (siloxane-based) were lower than those obtained for the unaged specimens (Figure 2b).

It is worth noting that the mechanisms of water penetration within the system by capillarity and under low pressure are different. Water penetration under low pressure is associated with larger pores (>10 μm) compared to capillary pores (1 to 10 μm) [3], which might indicate an expansion of the porous network (occlusion-destruction of capillary pores and increase in non-capillary pores). The increase in permeability under low pressure may also be associated with microcracks in the substrate (basecoat) that may result from the aging tests and may not be efficiently protected by the finishing coats, especially in the case of H1 and H3. Additionally, continuous water absorption and drying, associated to repeated volumetric changes, can also create internal mechanical stresses in the pore network of the cementitious basecoat, favoring the formation of microcracks and can further develop over time, affecting the finishing coat [20].

3.2. Drying

Figure 3 and Table 4 show the drying curves and the results of the initial drying rate (DR_1), the second drying rate (DR_2), and the drying index (*DI*) for untreated and treated specimens before and after aging.

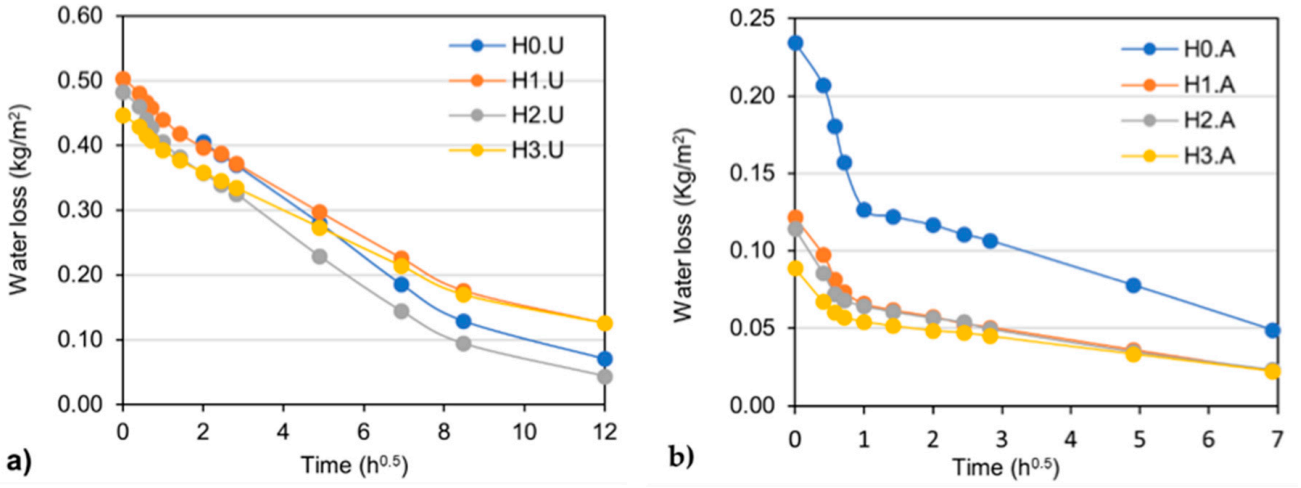

Figure 3. Drying curves of the (**a**) unaged and (**b**) aged specimens.

Table 4. Results of drying rate in the liquid phase (DR_1) and in the vapor phase (DR_2), drying index (DI), and total mass variation at the end of test (ΔTm), for treated/untreated specimens, prior to and after artificial aging test.

System	Unaged Specimens				Aged Specimens			
	DR_1 (kg/m^2·h)	DR_2 (kg/m^2·h$^{0.5}$)	DI	ΔTm (%)	DR_1 (kg/m^2·h)	DR_2 (kg/m^2·h$^{0.5}$)	DI	ΔTm (%)
H0 (reference)	0.062 ± 0.002	0.043 ± 0.001	0.125 ± 0.006	1.26 ± 0.08	0.106 ± 0.009	0.013 ± 0.003	0.193 ± 0.060	0.78 ± 0.47
H1	0.038 ± 0.003	0.035 ± 0.001	0.249 ± 0.025	2.06 ± 0.15	0.051 ± 0.017	0.008 ± 0.001	0.186 ± 0.035	0.33 ± 0.08
H2	0.046 ± 0.004	0.042 ± 0.001	0.110 ± 0.003	0.80 ± 0.17	0.043 ± 0.004	0.008 ± 0.001	0.202 ± 0.029	0.37 ± 0.09
H3	0.031 ± 0.001	0.030 ± 0.000	0.280 ± 0.026	2.32 ± 0.19	0.029 ± 0.005	0.005 ± 0.001	0.250 ± 0.056	0.35 ± 0.09

In general, it can be observed that all the hydrophobic products decreased both the initial and second drying rates. Moreover, it was found that the drying index increased with the application of the acrylic-based products H1 and H3 (99.3% and 123.7%, respectively, and considering the DI value obtained for H0) and, conversely, decreased with the application of the siloxane-based product H2 (12.4%). In fact, H2 had a lower impact on the drying rates (DR_1 and DR_2), keeping drying kinetics in the 2nd step of drying (DR_2) practically unchanged, whereas the acrylic-based treatments (H1, H3) induced a more significant alteration in the drying kinetics (higher delay, especially in the case of H3, with a 32% decrease in DR_2) (Table 4).

The aging effect was more evident in the drying rate 2 (DR_2), corresponding to the water vapor evaporation. After aging, the unprotected system suffered a DR_2 reduction of 71.1%, and the protected systems (H1, H2, and H3) suffered a reduction of about 80%.

According to the results presented in Table 4 (drying index before and after aging), it is possible to verify that artificial aging had a considerable impact on H0 and H2, with an increase in drying resistance of 54.0% and 83.4%, respectively. In contrast, the values of H1 and H3 decreased by 25.3% and 10.8% when compared to the values obtained for the unaged specimens.

Compared to the aged untreated system, aged H1 has a lower drying index (−3.4%) and aged H2 and H3 a higher DI (+4.7% and +29.5%, respectively). Even after artificial aging, H3 induced a higher delay in the drying of the substrate, whereas H1 and H2 presented negligible DI variations (Table 4).

3.3. Contact Angle

With the application of a water-repellent protection product, a reduction in water absorption and an increase in the contact angle of the protected surface (>90°) is expected [6]. In the present study, a significant reduction in water absorption both by capillarity and under low pressure was observed. However, although the application of H2 and H3 induced an increase in the contact angle (54.3% and 16.1%, respectively), a considerable θ reduction (32.7%) was observed with the application of H1 (Table 5, Figure 4). The decrease in the contact angle in this latter case can be related to the chemical composition of the product. In fact, H1 is a generic product with no specific water repellent properties stated in its technical data sheet. This product contains a higher amount of non-polymeric additives, such as fillers or pigments, if compared to H2 and H3. These additives confer hydrophilic properties to the product, explaining the decrease in the contact angle and the increase in the surface wettability. Additionally, it is worth noting that acrylic products can be functionalized using several monomers with specific characteristics [21]. Thus, it is possible to create acrylic (co)polymers with hydrophilic or hydrophobic properties [10].

On the other hand, an increase in the contact angle was observed after the application of H2 and H3, although the contact angles did not achieve the lower limit of hydrophobicity (90°) (Figure 4). In the case of H3, further percentages of acrylates (i.e., disobutyrate, butyl acrylate, methyl methacrylate), when compared to H1, can provide enhanced hydrophobic features [5]. Conversely, the inclusion of significant percentages of TiO_2 nanoparticles as pigments and/or self-cleaning additives [22] (up to 25% in volume, as indicated in the technical sheet of all products) generally provides hydrophilic properties. The addition

of inorganic additives (e.g., carbonates) to the paint formulation can also increase surface wetting and hygroscopicity, hence affecting contact angle values [23,24].

Table 5. Average results and relative standard deviation of contact angle (θ) of protected and unprotected specimens prior to and after artificial aging test.

System	Unaged Specimens θ (°)	Aged Specimens θ (°)
H0 (reference)	54 ± 8	85 ± 6
H1	37 ± 5	64 ± 5
H2	84 ± 8	111 ± 3
H3	63 ± 5	75 ± 5

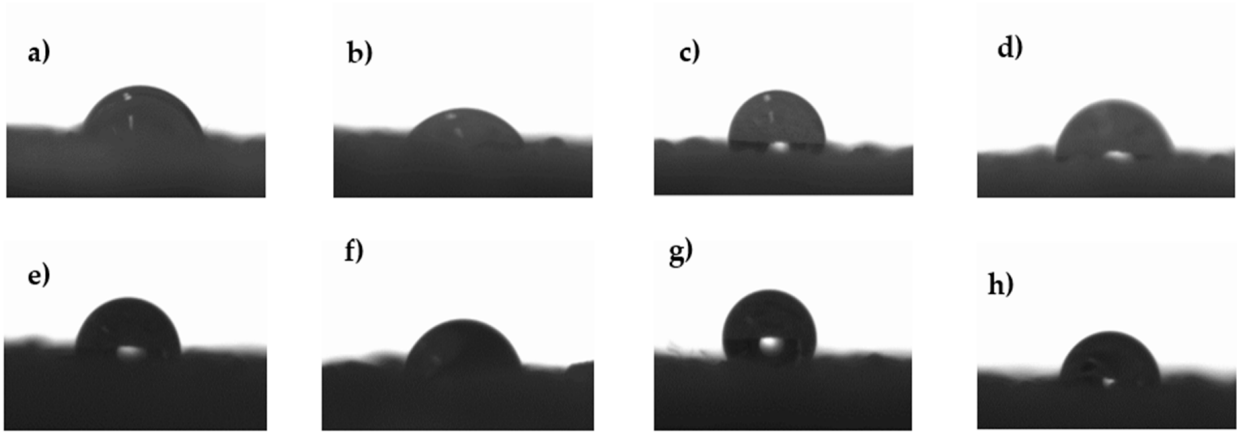

Figure 4. Contact angle of water droplets on (**a**) untreated Specimen, (**b**) H1, (**c**) H2 and (**d**) H3 before aging; (**e**) untreated Specimen, (**f**) H1, (**g**) H2 and (**h**) H3 after aging.

Following the trend observed for the capillary water absorption, the results of the contact angle increased for all systems after the artificial aging (Table 5). The highest increase (~73%) was obtained for H1 and the lowest (~19%) for H3. However, lower contact angle values were observed for the aged H1 and H3 specimens when compared to the aged reference (H0).

A contact angle >90° was observed only in the case of the aged H2 (Table 5), indicating a hydrophobic surface. However, this system has a slightly higher capillary water absorption result compared to H2 (Section 3.1.).

It is worth noting that the disagreement between the values of the contact angle and the capillary water absorption has already been verified in previous studies [25]. The values of the contact angle are only related to the drop-surface interface and evaluate an immediate water repellence behavior. On the other hand, the capillary water absorption provides an enhanced assessment of the long-term water resistance. Thus, it can be concluded that there is no clear linear correlation between the contact angle and the water absorption of a surface, especially when comparing multifunctional protection products (paints) with a complex formulation. Competitive effects between the polymeric component with hydrophobic properties and the titanium dioxide nanoparticles with hydrophilic (photocatalytic) features can also occur.

3.4. Water Vapor Permeability

The results showed that water vapor permeability slightly improves with the application of the H1 and H2 products. In fact, the water vapor diffusion resistance coefficient (μ) reduced (up to 4%) after H1 and H2 product application. On the other hand, a higher resistance to the diffusion of water vapor (14%) was observed with the application of H3 (Table 6). Similar results were found by Esteves et al. [7], where an increase in the μ-value between 4% and 21% was obtained after the application of three silicon-based hydrophobic

products to the ETICS. The water vapor diffusion resistance coefficient (μ) of the thermal insulation (EPS) was also obtained, and the results are in accordance with those presented by Parracha et al. [26]. Results also confirmed that all rendering systems have $S_d < 2$ m, thus respecting the requirement of EAD 040083-00-0404 [11] for ETICS certification (Table 6).

Table 6. Results of the water vapor permeability test for unprotected and protected specimens, before and after artificial aging.

System	μ EPS	Unaged Specimens		Aged Specimens	
		μ ETICS	S_d of the Rendering System (m)	μ ETICS	S_d of the Rendering System (m)
H0	39.07 ± 3.11	43.84 ± 0.10	0.35 ± 0.02	80.39 ± 10.25	1.93 ± 0.43
H1		43.65 ± 0.12	0.34 ± 0.01	65.14 ± 0.73	1.26 ± 0.02
H2		42.10 ± 2.95	0.26 ± 0.11	73.08 ± 10.48	1.61 ± 0.46
H3		50.04 ± 3.90	0.62 ± 0.18	103.02 ± 20.88	2.86 ± 0.92

After the artificial aging, the unprotected system (H0) underwent a significant permeability decrease (~80%), thus in accordance with the results of the drying test (DR_2). H1 and H2 have the most compatible values, with a moderate vapor permeability decrease, considering, also, that the products protected the system during the aging cycles. The product H3, as in the unaged specimens, showed a higher resistance to vapor diffusion compared to the untreated system. The S_d obtained for the aged H3 exceeds the recommended threshold value of 2 m, defined by EAD 040083-00-0404 [11]. However, the remaining systems (H0, H1, and H2) still present values of $S_d < 2$ m (Table 6). The results indicate that after aging and mainly for the system with the application of H3, interstitial condensations can easily occur, affecting the durability of the system [3].

3.5. Optical Microscopy

The surfaces of the treated and untreated ETICS specimens were observed through optical microscopy. Figure 5 presents the microphotographs of the untreated and treated specimens before and after aging.

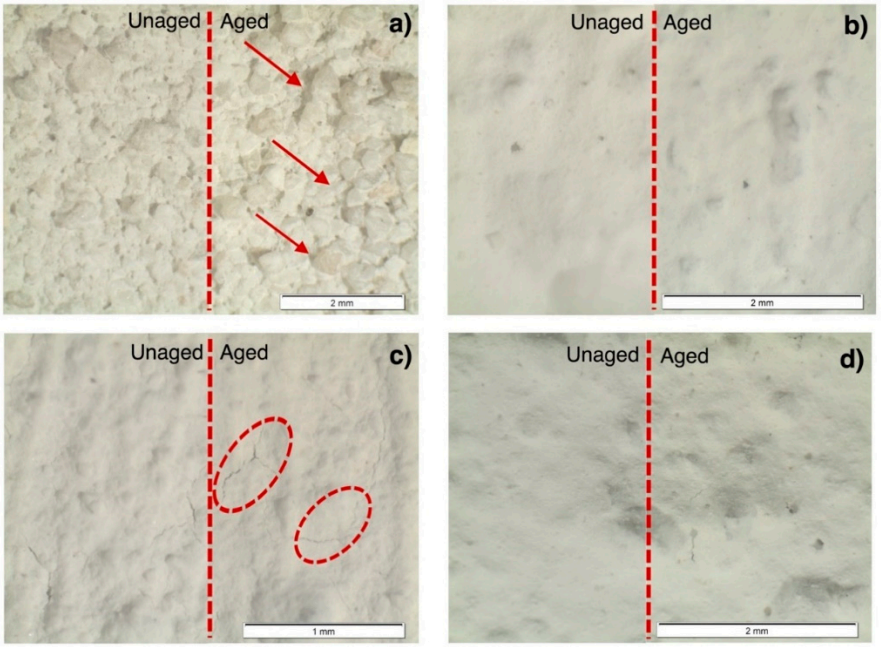

Figure 5. Microphotographs of (**a**) untreated and treated with (**b**) H1, (**c**) H2, (**d**) H3 ETICS, before and after artificial aging; the arrows and the dotted circles indicate particle decohesion and microcracks, respectively.

A reduction in surface roughness with the application of the protection products was generally observed. The protection films of products H1 and H3 (Figure 5b,d, respectively) have some micropores, while the film of H2 has microcracks (Figure 5c).

The surfaces of the untreated specimens were not significantly altered after the aging test. However, the surfaces of the finishing coat present some particle decohesion, whose formation can be attributed to the heat-cold and freeze-thaw cycles (Figure 5a).

Product H1 and H3, both acrylic-based, showed a significant amount of micropores and some microcracks along the paint film after aging (Figure 5b,d). On the other hand, the specimen treated with H2, based on siloxane resins, showed a considerably higher amount of microcracks (Figure 5c), as observed in Figure 1a.

3.6. Susceptibility to Mould Development

During the 4 weeks of testing, no mould development was observed in the systems, with or without extra protection (all specimens rated as 0). The results obtained after artificial aging also showed no mould development on the treated surfaces. Only one of the three untreated specimens was rated as 1 (<10% of the contaminated surface) after aging (Figure 6a).

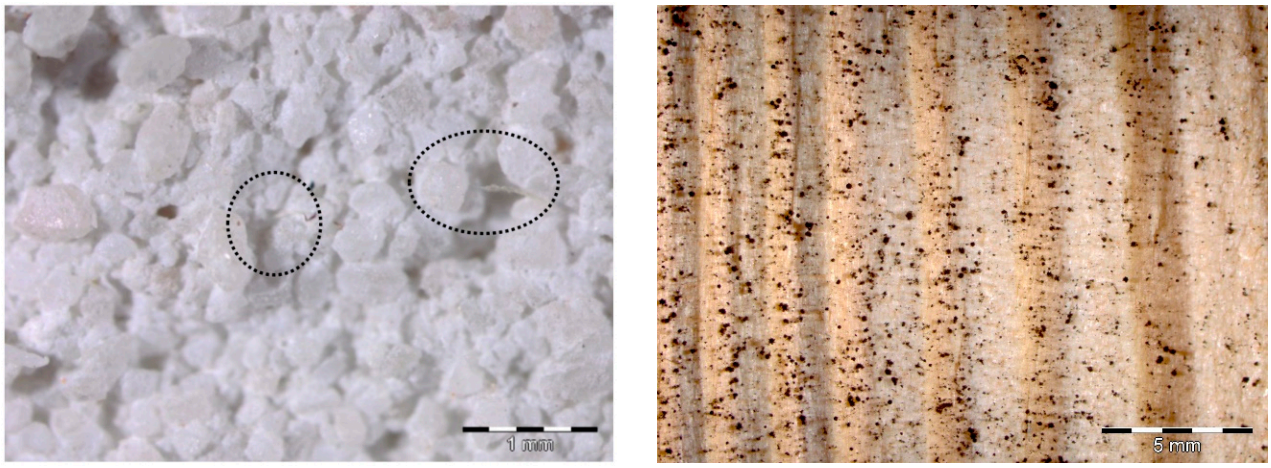

(**a**) (**b**)

Figure 6. Mould growth on (**a**) untreated specimen after aging and (**b**) control specimen. The dotted circles in Figure 6a indicate hyphae development.

The change of water absorption properties could be partially responsible for the full prevention of mould development on treated specimens. Nevertheless, the main bio-protection was most probably achieved by the biocides present on both the protective coatings and the finishing coat of the system.

The results obtained for the controls, all rated as four at the end of the test (Figure 6b), allowed the validation of the test procedure.

4. Discussion

An overview of the moisture transport properties of the untreated and treated substrates, prior to and after artificial aging, is shown in Figure 7. It is possible to verify that the application of the hydrophobic products generally induces a reduction in both the capillarity water absorption coefficient (C) and the water absorption coefficient under low pressure (C^{60}), being the substrate treated with H3 the less water-absorbent. After aging, there is a significant reduction in the water absorption coefficients, also in the case of the untreated ETICS.

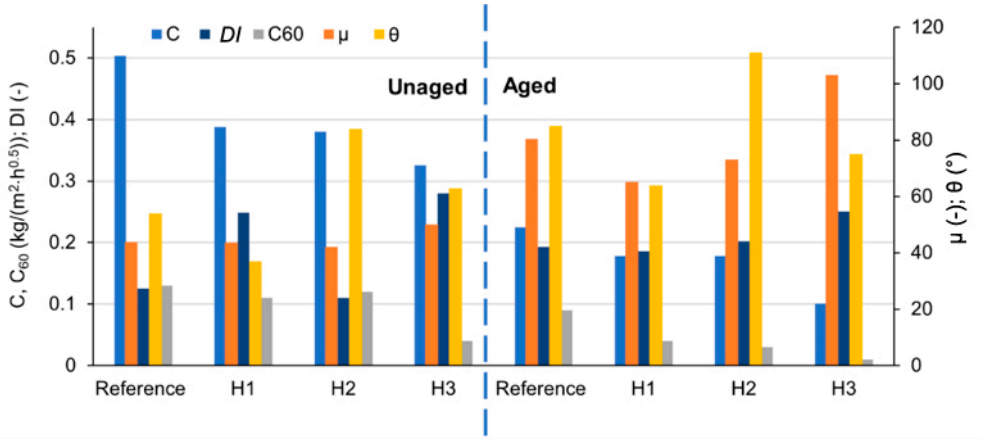

Figure 7. Moisture transport properties of (unaged and aged) untreated (reference) and treated (H1, H3: acrylic-based products H2: siloxane-based product) specimens, where C: water absorption coefficient by capillarity; C^{60}: water absorption coefficient under pressure; *DI*: drying index; μ: water vapor diffusion resistance factor; θ: contact angle.

The reduction of capillary water absorption after aging with hygrothermal cycles can be attributed to the possible alteration of the physical-chemical alteration of the polymeric matrix of the protective coatings, which leads to higher compactness and stiffness, thus, a higher tendency to microcracking. This behavior is mostly due to freeze-thaw cycles, which can also favor a loss of cohesion and material on the surface (as observed in Figure 5).

Furthermore, the porosity of the base layer of the ETICS can also be reduced by dissolution-reprecipitation processes of the cement basecoat or as a result of the evolution in the hydration reactions of the cement due to exposure to significant amounts of water in the aging cycles [3].

Previous studies, which considered the same type of artificial aging cycles in cement mortars [3,27], report similar results, i.e., less water permeability after aging cycles due to cement hydration as a result of freeze-thaw cycles. Additionally, Farinha et al. [28] and Oliveira et al. [27] found that, after the same aging cycles, mortars also had higher mechanical resistance. In fact, cement hydration can partially fill the porous network of the mortar, providing a more compact and, therefore, more durable microstructure [28].

In the case of treated specimens, a major cause for *Cc* increase is identified in the reduction of capillary suction, resulting from the expansion of capillary pores and as a consequence of micro-cracking (Figure 5).

Concerning the drying index, H1 and H3 (both acrylic-based products) induced a *DI* increase, with higher variations in the case of H3 (124%), whereas H2 induced a decrease in *DI*. After aging, the alterations in *DI* are reduced, if compared to the aged untreated system, with the highest value (+30%) being H3. H2 treatment, based on siloxane resins, was the product that least influenced the drying kinetics before and after aging of the ETICS. Although aging with H2 showed a slight impact on the surface (an increase in *DI*, Figure 7), compared to the unprotected surface, taking into account that the product also improved the water-repellent properties of the substrates, the variations in the drying process are negligible.

In the same test, the aging effect was more evident in DR_2, with a significant reduction in the speed of water vapor transport, i.e., DR_2 reduction (as observed in Table 3). This trend supports the hypothesis of a change in porosity due to the aging cycles, with a decrease in capillary pores (also justified by the lower amount of water absorbed), as well as smaller pores. In fact, the transport of water vapor occurs mainly in pores smaller than 0.1 μm, while the transport of liquid water, by capillarity, occurs mainly in pores in the range of 0.1–10 μm [29].

Regarding the WVP, H3 (acrylic-based product) showed a reduction in vapor permeability (14% compared to the untreated system), with a different trend compared to the other two products. After aging, all systems suffered a reduction in water vapor permeability (Figure 7), with a significant increase in diffusion resistance of the water vapor coefficient (μ), which is in accordance with a possible reduction in porosity of the ETICS due to the aging cycles. However, it is also verified that the application of H1 and H2 protected the system from the effects of aging, still maintaining compatible μ values.

H2 exhibited better performance in terms of water vapor permeability and DR_2 compared to H1; this trend can be attributed to the use of polymers (siloxane vs. acrylic) with different polymer microstructure, crosslink density, and morphology [30]. In fact, siloxane consists of short silicon atoms chains (3 to 8 atoms) and a molecular size of up to 7.5 nm [31]. The space between the silicon and oxygen atoms is larger than an individual water molecule (0.35 nm [31]), theoretically allowing the passage of water vapor through the polymeric structure. Furthermore, siloxane-based compounds have hydrophobic properties due to their nonpolar organic groups (usually alkoxy groups, e.g., methyl (CH_3)), propyl (C_3H_7), and octyl (C_8H_{17})), which repel polar OH^- groups of water [32].

Additionally, other characteristics of the paints, such as the binder content, the size, and the morphology of the pigment, have an influence on the permeability of the protective films. Topçuoğlu et al. [33] found that the permeability of water-based acrylic paints containing different binder amounts dramatically decreased with increasing binder content. This behavior was explained by the formation of a porous structure as the binder content decreased from 40% to 10%.

The contact angle values of the treated surfaces can also be influenced by other factors. The presence of titanium dioxide (TiO_2) and zinc oxide (ZnO) nanoparticles, which have hydrophilic properties, can justify the low values obtained for the contact angle.

5. Conclusions

This study focused on the analysis of the hydrophobic features provided by three commercial paints (two acrylic-based and one siloxane-based) when applied to ETICS solutions. The moisture transport properties and susceptibility to mould development were assessed through laboratory tests on untreated and treated specimens. The durability of the treatments was also evaluated through artificial aging tests (heat-cold and freeze-thaw cycles).

It was concluded that the hydrophobic protection product H2, based on siloxane, presented a slightly better performance than the H1 and H3 acrylic-based products. H2 showed the lowest variation in the drying kinetics of the ETICS, before and after aging, as well as the most suitable vapor permeability in the initial performance, with a negligible alteration of the substrate vapor permeability after aging. Additionally, H2 obtained the highest contact angle values (111°) after aging, classifying this product as hydrophobic, considerably higher than those of the acrylic-based products. However, acrylic-based product H3 presented the lowest values for capillary water absorption, even after aging.

Regarding biological susceptibility, neither treated nor untreated substrates showed significant biological growth, either before or after accelerated artificial aging. This positive behavior is mainly attributed to the amount of biocide present in the formulations of the finishing products.

Hygrothermal cycles only slightly affect the water transport properties of the analyzed systems, inducing even lower water absorptions and higher contact angles. A slight increase in the water absorption was observed only in the Karsten tubes test, mainly in the case of the specimens treated with (acrylic-based) H1 and H3. Even after aging, the protection systems continued to show a higher water repellency than the untreated ETICS.

However, the aging cycles significantly affected the drying and vapor permeability of the systems. Concerning water vapor permeability, products H1 and H2 contributed to a higher permeability of the aged, treated specimens than the untreated system. Conversely,

specimens treated with H3 (acrylic-based) showed significantly lower DR_2 and higher resistance to drying (*DI*) before and after accelerated aging. However, it is worth noting that no significant water amount is retained in all the treated systems.

Considering that the (hygrothermal) aging cycles provided less water absorption, higher resistance to drying, and less water vapor permeability of the untreated system, the aging cycles possibly affect the porosity of the ETICS, i.e., cause a reduction of the porosity of the system.

In general, it can be concluded that the hydrophobic protection products are suitable for the repair or protection of the ETICS. Product H2 (based on siloxane) is the most compatible with the ETICS, respecting the drying kinetics and permeability of the system. H1 also showed moderate compatibility; however, H3 can induce a considerable alteration to the drying and water vapor permeability of the ETICS. In fact, H3 is the most waterproof product, both to liquid water and water vapor.

It is worth noting that the H1 protection product performed properly as a hydric protection coating in the ETICS, despite being a generic commercial paint, with no specific water repellent properties, as in the case of the other two studied paints.

The present study concluded that the considered water-repellent products could efficiently increase the durability of the ETICS with a cement basecoat and an acrylic-based finishing coat.

Research is ongoing to further correlate the physical properties (e.g., pore size distribution) of the treated substrate to the effect of the hydrophobic products, as well as to assess the performance of the products when exposed to other degradation agents, such as UV radiation and pollutants.

Author Contributions: Conceptualization, R.R., G.B., I.F.-C. and R.V.; Data curation, R.R. and J.L.P.; Formal analysis, G.B. and J.L.P.; Funding acquisition, I.F.-C. and R.V.; Investigation, R.R.; Project administration, I.F.-C. and R.V.; Software, R.R. and G.B.; Supervision, G.B., J.L.P., I.F.-C. and R.V.; Validation, G.B., I.F.-C., R.V. and L.N.; Visualization, R.R. and G.B.; Writing–original draft, R.R.; Writing–review & editing, G.B., J.L.P., I.F.-C., R.V. and L.N. All authors have read and agreed to the published version of the manuscript.

Funding: This research was funded by Portuguese Foundation for Science and Technology (FCT) within research project PTDC/ECI-EGC/30681/2017 (WGB_Shield—Shielding building' façades on cities revitalization. Triple resistance for water, graffiti and biocolonization of external thermal insulation systems) and for the scholarship 2020.05180.BD (J. L. Parracha).

Institutional Review Board Statement: Not applicable.

Informed Consent Statement: Not applicable.

Acknowledgments: The authors also acknowledge the company Robbialac for the supply of the products, as well as Pedro Nolasco from NanoMatLab (CQE research unit, IST) for contact angle measurements.

Conflicts of Interest: The authors declare no conflict of interest.

References

1. Energy Performance of Building Directive (EPBD). Directive 2010-31-EU of the European Parliament and of the Council. *Off. J. Eur. Union* **2010**, *153*, 13–34.
2. Barreira, E.; Freitas, V.P. Experimental study of the hygrothermal behaviour of external thermal insulation composite systems (ETICS). *Build. Environ.* **2013**, *63*, 31–39. [CrossRef]
3. Borsoi, G.; Esteves, C.; Flores-Colen, I.; Veiga, R. Effect of hygrothermal aging on hydrophobic treatments applied to building exterior claddings. *Coatings* **2020**, *10*, 363. [CrossRef]
4. Silva, L.; Flores-Colen, I.; Veira, N.; Timmons, A.B.; Sequeira, P. Durability of ETICS and Premixed One-Coat Renders in Natural Exposure. In *New Approaches to Building Pathology and Durability, Building Pathology and Rehabilitation*; Delgado, J.M.P.Q., Ed.; Springer: Singapore, 2016; Volume 6, pp. 131–158.
5. Bader, T.; Waldner, B.J.; Unterberger, S.H.; Lackner, R. On the performance of film formers versus penetrants as water-repellent treatment of high-performance concrete (HPC) surfaces. *Constr. Build. Mater.* **2019**, *203*, 481–490. [CrossRef]

6. Ferreira Pinto, A.P.; Delgad Rodrigues, J. Effectiveness and Stability Over Time of Water Repellent Treatments on Carbonate and Granitic Stones. In *Hydrophobe VII—7th International Conference on Water Repellent Treatment and Protective Surface Technology for Building Materials*; Elena Charola, A., Delgado Rodrigues, J., Eds.; LNEC (Laboratório Nacional de Engenharia Civil): Lisbon, Portugal, 2014; pp. 151–160.
7. Esteves, C.; Ahmed, H.; Flores-Colen, I.; Veiga, R. The influence of hydrophobic protection on building exterior claddings. *J. Coat. Technol. Res.* **2019**, *16*, 1379–1388. [CrossRef]
8. McGettigan, E. Factors affecting the selection of water-repellent treatments. *APT Bull. J. Preserv. Technol.* **1995**, *26*, 22–26. [CrossRef]
9. Levi, M.; Ferro, C.; Regazzoli, D.; Dotelli, G.; Lo presti, A. Comparative evaluation method of polymer surface treatments applied on high performance concrete. *J. Mater. Sci.* **2002**, *37*, 4881–4888. [CrossRef]
10. Sabatini, V.; Pargoletti, E.; Longoni, M.; Farina, H.; Ortenzi, M.A.; Cappelletti, G. Stearyl methacrylate co-polymers: Towards new polymer coatings for mortars protection. *Appl. Surf. Sci.* **2019**, *488*, 213–220. [CrossRef]
11. EOTA. *European Assessment Document EAD 040083-00-0404–External Thermal Insulation Composite Systems (ETICS) with renderings*; European Organization for Technical Approvals: Brussels, Belgium, 2019.
12. CEN—European Committee for Standardization. *Conservation of Cultural Heritage—Test Methods—Determination of Drying Properties*; EN 16322; CEN: Brussels, Belgium, 2013.
13. RILEM. Water Absorption Under Low Pressure. In *Pipe Method*; Test N II.4; Tentative Recommendations: Paris, France, 1980.
14. CEN—European Committee for Standardization. *Methods of Methods of Test for Mortar for Masonry—Part 19: Determination of Water Vapour Permeability of Hardened Rendering and Plastering Mortars*; EN 1015-19; CEN: Brussels, Belgium, 2008.
15. ASTM. *Determining the Resistance of Paint Films and Related Coatings to Fungal Defacement by Accelerated Four-Week Agar Plate Assay*; ASTM D5590-17:2017; ASTM International: Pennsylvania, PA, USA, 2017.
16. ASTM. *Standard Test Method for Determining Fungi Resistance of Insulation Materials and Facings*; ASTM C1338-19:2019; ASTM International: Pennsylvania, PA, USA, 2019.
17. Parracha, J.L.; Cortay, A.; Borsoi, G.; Veiga, M.R.; Nunes, L. Evaluation of ETICS Characteristics That Affect Surface Mould Development. In *XV International Conference on Durability of Building Materials and Components—DBMC 2020*; Serrat, C., Casas, J.R., Gibert, V., Eds.; Universitat Politècnica de Catalunya: Barcelona, Spain, 2020; pp. 191–200.
18. CEN—European Committee for Standardization. *Methods of Test for Mortar for Masonry—Part 18: Determination of Water Absorption Coefficient due to Capillary Action of Hardened Mortar*; EN 1015-18; CEN: Brussels, Belgium, 2002.
19. Maia, J.; Ramos, N.M.M.; Veiga, R. Assessment of test methods for the durability of thermal mortars exposure to freezing. *Mater. Struct.* **2019**, *52*, 112. [CrossRef]
20. Ergenç, D.; Sierra-Fernandez, A.; Barbero-Barrera, M.M.; Gomez-Villalba, L.S.; Fort, R. Assessment on the performances of air lime-ceramic mortars with nano-$Ca(OH)_2$ and nano-SiO_2 additions. *Constr. Build. Mater.* **2020**, *232*, 117163. [CrossRef]
21. Bader, T.; Unterberger, S.H.; Lackner, R. Effect of substrate moisture on the weatherability of surface treatment for high-performance concrete (HPC). *Cem. Concr. Compos.* **2017**, *83*, 57–65. [CrossRef]
22. Quagliarini, E.; Bondioli, F.; Goffredo, G.B.; Licciulli, A.; Munafo, P. Self-cleaning materials on architectural heritage: Compatibility of photo-induced hydrophilicity of TiO_2 coatings on stone surfaces. *J. Cult. Herit.* **2013**, *14*, 1–7. [CrossRef]
23. Féat, A.; Federle, W.; Kamperman, M.; Murray, M.; Van der Gucht, J.; Taylor, P. Slippery paints: Eco-friendly coatings that cause ants to slip. *Prog. Org. Coat.* **2019**, *135*, 331–334. [CrossRef]
24. Jiang, W.; Jin, X.; Li, H.; Zhang, S.; Zhou, T.; Xie, H. Modification of nano-hybrid silicon acrylic resin with anticorrosion and hydrophobic properties. *Polym. Test.* **2020**, *82*, 106287. [CrossRef]
25. La Russa, M.F.; Rovella, N.; Alvarez de Buergo, M.; Belfiore, C.M.; Pezzino, A.; Crisci, G.M.; Ruffolo, A. Nano-TiO_2 coatings for cultural heritage protection: The role of the binder on hydrophobic and self-cleaning efficacy. *Prog. Org. Coat.* **2016**, *91*, 1–8. [CrossRef]
26. Parracha, J.L.; Borsoi, G.; Flores-Colen, I.; Veiga, R.; Nunes, L.; Dionísio, A.; Glória Gomes, M.; Faria, P. Performance parameters of ETICS: Correlating water resistance, bio-susceptibility and surface properties. *Constr. Build. Mater.* **2021**, *272*, 121956. [CrossRef]
27. Oliveira, R.; De Brito, J.; Veiga, R. Incorporation of fine glass aggregates in renderings. *Constr. Build. Mater.* **2013**, *44*, 329–341. [CrossRef]
28. Farinha, C.; De Brito, J.; Veiga, R. Incorporation of fine sanitary ware aggregates in coating mortars. *Constr. Build. Mater.* **2015**, *83*, 194–206. [CrossRef]
29. Xiong, H.; Yuan, K.; Wen, M.; Yu, A.; Xu, J. Influence of pore structure on the moisture transport property of external thermal insulation composite system as studied by NMR. *Constr. Build. Mater.* **2019**, *228*, 116815. [CrossRef]
30. Pan, X.; Shi, Z.; Shi, C.; Ling, T.; Li, N. A review on concrete surface treatment Part I: Types and mechanisms. *Constr. Build. Mater.* **2017**, *132*, 578–590. [CrossRef]
31. Kus, H. Long-Term Performance of Water Repellants on Rendered Autoclaved Aerated Concrete. Ph.D. Thesis, Centre For Built Environment, University of Gävle, Royal Institute of Technology, Stockholm, Sweden, 2002.
32. Selley, D. Chemical considerations for making low-VOC silicon-based water repellents. *J. Coat. Technol. Res.* **2010**, *7*, 26–35.
33. Topçuoğlu, Ö.; Altinkaya, S.A.; Balköse, D. Characterization of waterborne acrylic based paint films and measurement of their water vapor permeabilities. *Prog. Org. Coat.* **2006**, *56*, 269–278. [CrossRef]